ARTICLES

Effect of Molecular Rotation on the Atomic Alignment Dependence in the Oriented Ar ($^3P_2$) + CF$_3$H Reaction

D. Watanabe, H. Ohoyama,* T. Matsumura, and T. Kasai

Department of Chemistry, Graduate School of Science, Osaka University Toyonaka, Osaka 560-0043, Japan

Received: May 2, 2007; In Final Form: June 1, 2007

Atomic alignment effect for the CF$_3$* formation in the oriented Ar ($^3P_2$, $M_J = 2$) + CF$_3$H reaction has been investigated at different two CF$_3$H beam conditions: effusive and supersonic beams. The chemiluminescence intensity of CF$_3$* was measured as a function of the magnetic orientation field direction in the collision frame. A significant contribution of rank 4 moment was recognized. The cross-section for each magnetic M'_J substate in the collision frame, $\sigma^{|M'_J|}$, was determined to be $\sigma^{|M'_J|=0}:\sigma^{|M'_J|=1}:\sigma^{|M'_J|=2} = 1.00:0.84 \pm 0.02:0.88 \pm 0.02$ for the effusive CF$_3$H beam condition. The atomic alignment effect was found to significantly depend on the CF$_3$H beam condition. For the supersonic beam condition, $\sigma^{|M'_J|=0\&1}$ was changed to be smaller than $\sigma^{|M'_J|=2}$.

1. Introduction

The scattering process involving aligned states of atoms is one of the well-explored fields of study.[1−6] So far, it has been recognized that the atomic alignment effect on the scattering processes in the singlet and/or doublet states is dominantly determined by only the orbital angular momentum L and its projection L_Z as the so-called the "Percival−Seaton hypothesis" that the electronic spin has little influence on the dynamics.[7] However, it is not obvious that this kind of stereoselectivity is of general relevance for the systems with different spin multiplicity. So far, little is known about the atomic alignment effect for the triplet species. Recently, we have developed an oriented Ar ($^3P_2$, $M_J = 2$) beam and apply it to the dissociative energy transfer reaction for Ar ($^3P_2$) + N$_2$,[8] (N$_2$O)$_n$, (H$_2$O)$_n$,[9] CH$_3$CN (CD$_3$CN),[10] and (CH$_3$CN)$_2$, (CD$_3$CN)$_2$,[11] and revealed the atomic alignment effects depending not only on the orbital angular momentum L (and its projection L_Z) but on the total angular momentum J (and its projection M_J) involving spin effect unique to the triplet species. Moreover, we have suggested the selectivity of the final excited states depending on the atomic M'_J substate in the collision frame. To study how the unpaired inner orbital of the triplet species interacts with the outer extended orbital in the course of energy transfer process, it is of great importance to compare the atomic alignment effect with the effect on the molecular orientation in the same reaction system because the energy transfer reaction should be controlled by the mutual configuration of two reactants.

For the title reaction, we have studied the molecular orientation dependence for the CF$_3$* formation by using the oriented CF$_3$H beam.[12−16] On the basis of the steric opacity function, we have suggested the important contribution of the 6a$_1$ molecular orbital (MO) of CF$_3$H. Because the effect of molecular orientation has been studied, it is of great interest to compare the atomic alignment effect with the effect on the molecular orientation in this reaction system.

The cross-section of CF$_3$* formation in the CF$_3$H + Ar ($^3P_2$) reaction has been determined to be a few Å^2.[12] However, the total quenching cross-section of Ar ($^3P_2$) by CF$_3$H has been determined to be 64 Å^2 in the nearly thermal energy region.[17] The comparison of the cross-section for CF$_3$* formation with the total quenching cross-section gives an estimation of the low branching fraction to CF$_3$* formation. The main channel of the title reaction is estimated to be the H-elimination without emission. It has been known that several excited states relevant to the 6a$_1$ MO correlate to the CF$_3$* formation channel.

In the present study, we study the atomic alignment effect in the reaction of Ar ($^3P_2$) + CF$_3$H by using the oriented Ar ($^3P_2$) beam. A significant atomic alignment effect is observed. In addition, the atomic alignment effect is found to significantly depend on the CF$_3$H beam condition. The atomic alignment effect is discussed by comparing with the molecular orientation effect.

2. Experiment

The experimental apparatus and procedure were almost same as the previous one.[8] A metastable Ar ($^3P_{0, 2}$) beam generated by a pulsed glow discharge with a pulse width of 100 μs was state-selected by a magnetic hexapole. The almost pure Ar ($^3P_2$, $M_J = 2$) (more than 93%) beam collides with the CF$_3$H beam under different two beam conditions; effusive and supersonic beams, in a homogeneous magnetic orientation field. For the effusive beam, the CF$_3$H beam was injected with a stagnation pressure of 15 Torr from a pulsed valve that was placed at a distance of 8 cm from the beam crossing point. For the supersonic beam, the CF$_3$H beam was injected from a pulsed valve with a stagnation pressure of 400 Torr, and state selected by a 40 cm-long electrostatic hexapole to remove the contribution of clusters and to identify the rotational temperature. After state selection, the CF$_3$H beam was collided with the Ar ($^3P_2$, $M_J = 2$) at the beam crossing point. The detail of the electric
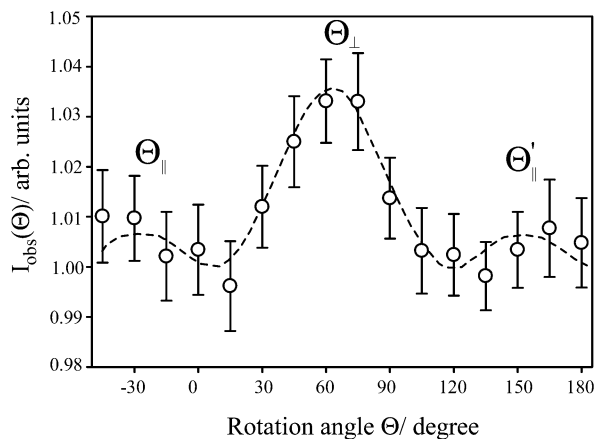
Figure 1. Θ-dependence of the CF$_3$* chemiluminescence intensity at the effusive CF$_3$H beam condition. The Θ-dependence reproduced by eq 3 is shown as a broken line.

hexapole state-selector was described elsewhere.[14,18] The visible chemiluminescence from the product CF$_3$* was selectively collected and detected by a suitable band-pass filter ($\lambda_C = 600$ nm). The signal from the photomultiplier was counted by a multichannel scaler (Stanford SR430). The chemiluminescence was measured as a function of the direction of the magnetic orientation field in the laboratory frame (rotation angle Θ). The origin of Θ is the direction of the Ar ($^3P_2$) beam axis. The homogeneous magnetic orientation field was generated by the four pieces of ferrite magnets mounted on a motor driven rotatable stage and its direction **B** was rotated around the beam crossing point over the angle region $-45 \leq \Theta \leq 180°$ by an interval of 15°.

3. Results and Discussion

3.1. M'_J-Dependent Cross-Section in the Collision Frame, $\sigma^{|M'_J|}$. Figure 1 shows the Θ-dependence of the CF$_3$* chemiluminescence intensity at the effusive beam condition measured as a function of the rotation angle Θ of the direction of magnetic orientation field **B**. This Θ-dependence can be analyzed using the evolution procedure based on an irreducible representation of the density matrix.[8] The chemiluminescence intensity, $I_{obs}(\Theta)$, can be written as follows by using the relative cross-section, $\sigma^{|M'_J|}$, in the collision frame.

$$I_{obs}(\Theta) = \frac{I(\Theta)}{DI} = \frac{1}{280}(39\sigma^{M_J=0} + 88\sigma^{|M'_J|=1} + 153\sigma^{|M'_J|=2}) +$$
$$\frac{1}{16}(-3\sigma^{M_J=0} - 4\sigma^{|M'_J|=1} + 7\sigma^{|M'_J|=2})\cos 2\theta + \frac{1}{64}(3\sigma^{M_J=0} -$$
$$4\sigma^{|M'_J|=1} + \sigma^{|M'_J|=2})\cos 4\theta \quad (1)$$

This equation is equivalent to the general multipole moment's form,

$$I(\Theta) = a_0 + a_2 \cos 2\theta + a_4 \cos 4\theta \quad (2)$$

where θ is the angle between the relative velocity v_R and the direction of the orientation magnetic field **B**. It is defined as $\theta \equiv \Theta_{v_R} - \Theta$ using the direction of the relative velocity v_R in the laboratory coordinate, Θ_{v_R}. Because θ has a distribution by the misalignment caused by the velocity distribution of CF$_3$H beam, we must use the cos $2n\theta$ factors averaged over the Maxwell–Boltzmann velocity distribution of CF$_3$H beam at room temperature, $\langle\cos(2n(\Theta_{v_R} - \Theta))\rangle$. We finally use the following equation for the evaluation of the experimental results,

$$I_{obs}(\Theta) = a_0 + a_2\langle\cos(2(\Theta_{v_R} - \Theta))\rangle + a_4\langle\cos(4(\Theta_{v_R} - \Theta))\rangle \quad (3)$$

The coefficients, a_n, were determined as the fitting parameters by the fitting using eq 3 by means of χ^2 analysis. They are summarized as follows:

$$a_2/a_0 = (14.1 \pm 1.57) \times 10^{-3}$$
$$a_4/a_0 = (8.95 \pm 2.04) \times 10^{-3}$$

A notable contribution of rank 4 moment (a_4) was recognized. This result strongly suggests that the unpaired inner orbital of the triplet species interacts with the outer extended orbital in the course of energy transfer process. These coefficient ratios were used to derive the relative cross-sections for each M'_J state, $\sigma^{M_J=0}$, $\sigma^{|M'_J|=1}$, and $\sigma^{|M'_J|=2}$. The $\sigma^{|M'_J|}$ for the effusive beam condition were determined to be $\sigma^{M_J=0}:\sigma^{|M'_J|=1}:\sigma^{|M'_J|=2} = 1.00: 0.84 \pm 0.02:0.88 \pm 0.02$. They were summarized in Figure 2. As a reference, the expected $\sigma^{|M'_J|}$ from the Percival–Seaton hypothesis were also shown in Figure 2 as a broken line that were calculated by using the standard recoupling procedure of angular momentum through the Clebsch–Gordan coefficients.[8,19] At a glance, it is recognized that the experimental $\sigma^{|M'_J|}$ does not follow the Percival–Seaton hypothesis. In addition, as for the alignment effect of p-orbital, it was found that the reactivity of $|L_Z| = 1$ configuration is almost equal to that of $L_Z = 0$ configuration. This result also conflicts with the theoretical expectation on the favorability of $L_Z = 0$ configuration for the electron exchange.[20] These results strongly indicate that the energy transfer process cannot be simply explained by the electron exchange model.

3.2. Characteristics of Potential Energy Surface. To understand the dynamical effect on the stereoselectivity, we have to know about the potential energy surface (PES) for Ar ($^3P_2$) + CF$_3$H. Unfortunately, it is difficult to obtain reliable interaction energy by the ab initio treatments of Ar ($^3P_2$) associated with highly excited electronic states. Because Ar ($^3P_2$) has the same outer valence electronic configuration as the K-atom with a 4s electron that mainly contributes to the interactions, the similarity between Ar ($^3P_2$) and the K-atom is expected.[21] For the qualitative understanding of the interaction potential for Ar ($^3P_2$) + CF$_3$H, we roughly calculated the model potential K + CF$_3$H by using a ground state K-atom instead of an Ar ($^3P_2$). The calculations are performed by the Hartree–Fock method with the 6-31++G(d,p) basis set. The potential energy V is obtained in the following manner:

$$V = E_{(K+CF_3H)} - (E_K + E_{CF_3H})$$

$E_{(K+CF_3H)}$, E_K, and E_{CF_3H} are the total energy of the supermolecule (K–CF$_3$H), the isolated K-atom, and the isolated CF$_3$H, respectively. The calculated model PES is shown in Figure 3A. Although the PES is attractive in all directions, the CF$_3$-group is more attractive than that around the H-end. To check the effect of BSSE (basis set superposition errors) on the qualitative characteristics of PES, the qualitative characteristics of PES was checked by an additional calculation of PES along the CF$_3$H axis ($Y = 0$) using the 6-311++G(3df,2pd) basis set (Figure 3B). In addition, we calculated the distribution of the "exterior electron" for the $6a_1$ MO of CF$_3$H by using the GAUSSIAN 98 ab initio program package with the 6-311++G(3df,2pd) basis set. The calculated electron density distribution of $6a_1$ MO is shown in Figure 4, and the "exterior electron" is shown as the shaded area. In addition, the van der Waals radius as an
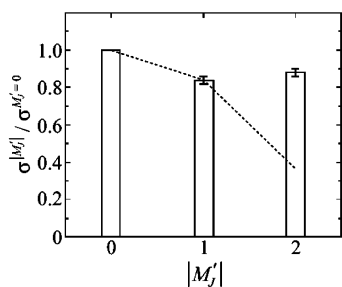
Figure 2. M'_J-resolved relative cross-section of Ar ($^3P_2$) + CF$_3$H. The broken line indicates the cross-sections estimated on the basis of the Percival−Seaton hypothesis.
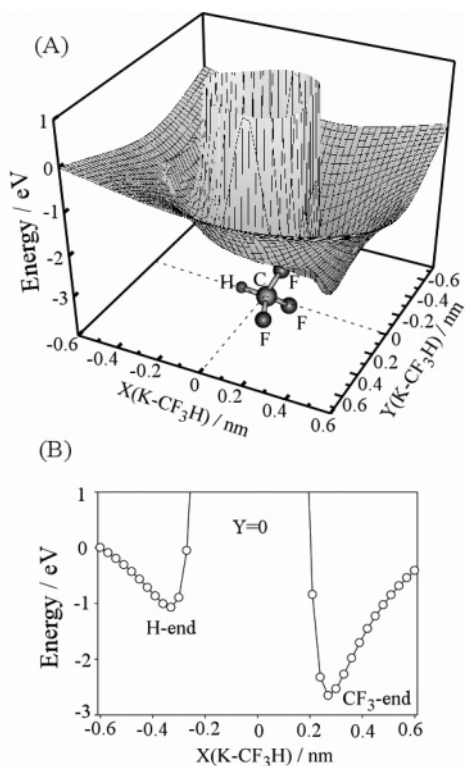

Figure 3. (A) Model potential energy surface of the Ar ($^3P_2$) + CF$_3$H reaction calculated by using the GAUSSIAN 98 ab initio program package with the 6-31++G(d,p) basis set under the condition where the 4s of Ar ($^3P_2$) is approximated by the corresponding K atom. The X-axis is the distance between C-atom and K-atom along the molecular axis of CF$_3$H. The Y-axis is the distance between C-atom and K-atom along the axis perpendicular to the molecular axis of CF$_3$H. (B) Cross-sectional view of PES along the CF$_3$H axis ($Y = 0$) calculated by using 6-311++G(3df,2pd) basis set.

approximate position of the repulsive wall (broken lines) is also shown in Figure 4.[22]

The energy transfer is expected to proceed via the following electron-exchange process:

Step 1. The electron in the 6a$_1$ orbital of CF$_3$H transfers to the half-filled 3p orbital of Ar ($^3P_2$).

Step 2. The 4s electron of Ar ($^3P_2$) transfers to the empty Rydberg orbital of CF$_3$H.

If the interaction between 3p and 4s is ignorable, the transition matrix element is given by[20,23,24]

$$V_{if} = \langle \varphi_i | H | \varphi_f \rangle \approx \langle 3p(1)Ryd(2)|1/r_{12}|MO(1)4s(2)\rangle$$

where H_{el} is the electronic Hamiltonian, and φ_i and φ_f are electronic wavefunctions for the initial and the final states, respectively, 4s and MO are the 4s orbital of Ar ($^3P_2$) and the
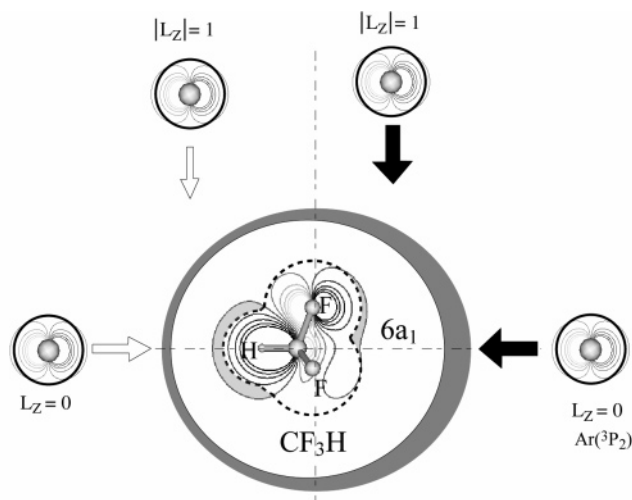

Figure 4. Electron density distribution of the 6a$_1$ molecular orbital of CF$_3$H calculated by the GAUSSIAN 98 program package with the 6-311++G(3df,2pd) basis set. The bold dashed line indicates the van der Waals surface of molecule as an approximate position of the repulsive wall, and the shaded area indicates the distribution of the "exterior electron" of the 6a$_1$ orbital. The arrows indicate the representative collision directions for most favorable collision (black arrows) and for favorable collision (white arrows).

molecular orbital of CF$_3$H in the initial states, respectively, and 3p and Ryd are the 3p orbital of Ar and the orbital of CF$_3$H in the final state, respectively. On the basis of the Mulliken approximation for the two-electron integral,[23] the steric effect for the transition matrix is approximated by the probability of orbital overlap.[24] Especially, we must consider the orbital overlap between the 3p orbital of Ar ($^3P_2$) and the 6a$_1$ orbital of CF$_3$H in step 1 because step 2 is expected to be more isotropic than step 1. On the basis of the simple consideration about characteristics of the PES and the distribution of the "exterior electron" of the 6a$_1$ orbital, we can deduce the interaction between the 6a$_1$ orbital and the 3p orbital of Ar ($^3P_2$). The collision from the CF$_3$-group is expected to be most reactive due to the deeper attractive well. This expectation agrees with the most reactive site at the CF$_3$-end in the molecular steric opacity function.[14] According to the exterior electron density model for the 6a$_1$ orbital,[22] this reaction is expected to have two reactive sites along the molecular symmetry axis. In this case, the $L_Z = 0$ configuration of the 3p orbital should be favorable for the collinear approach from both the CF$_3$-end and H-end directions. However, we have observed three reactive sites in the molecular steric opacity function; CF$_3$-end, H-end, and sideways.[14] Moreover, the observed atomic alignment dependence is a little anisotropic. From these points of views, we can assume that the $|L_Z| = 1$ configuration from the sideways direction is also favorable for the reaction. This assumption is in good agreement with both the characteristics of the molecular steric opacity function having three reactive sites and the slight atomic alignment dependence.

3.3. Effect of Molecular Rotation. Figure 5 shows the Θ-dependence measured under different two CF$_3$H beam conditions. At a glance, it is found that the Θ-dependence is significantly changed by the CF$_3$H beam condition. For the effusive beam, the reactivity at the Θ$_\perp$ configuration is larger than those at Θ$_\parallel$ and Θ$'_\parallel$, whereas for the supersonic beam, the reactivity at Θ$_\perp$ configuration is smaller than those at Θ$_\parallel$ and Θ$'_\parallel$. Because the M'_J state distribution at each configuration can be expressed by the $|d_{2,}^{M'_J}(\theta)|^2$ factors using Wigner d-function;[19] the Θ$_\parallel$ and Θ$'_\parallel$ configurations consist of almost pure $M'_J = 2, -2$ states, respectively. On the other hand, $|M'_J| = 0, 1$
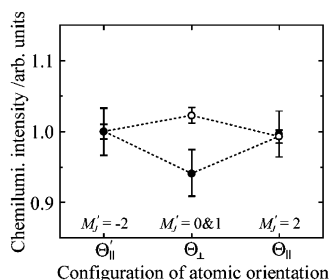
Figure 5. Θ-dependence of the CF$_3$* chemiluminescence intensity in the Ar (^{3}P$_2$, $M_J = 2$) + CF$_3$H reaction under two different CF$_3$H beam conditions: the effusive beam (open circle) and the supersonic beam (filled circle).

TABLE 1: Rotational State Distribution for the Effusive Beam and the Supersonic Beam of CF$_3$H

	effusive beam (15 Torr)	supersonic beam (400 Torr)
$T_{rot.}$ (K)	298	25
$\langle J \rangle$	23.6	8.64
$\langle K \rangle$	13.9	6.21

states coexist with an r atio of approximately 1:1 at the $\Theta_\perp$ configuration.

There are two possibilities for the origin of the different Θ-dependence on CF$_3$H beam condition. One is the effect of collision energy. Another is the effect of rotation of CF$_3$H.

The collision energy at the supersonic beam is slightly higher than that at the effusive beam. The collision energy is estimated to be $(8.0 \pm 1.5) \times 10^{-2}$ eV for the effusive beam and $(1.0 \pm 0.1) \times 10^{-1}$ eV for the supersonic beam, respectively. On the basis of the efficiency of the orbital overlap, the configuration of $L_Z = 0$ is favorable for the collision with small impact parameter, and the configuration of $|L_Z| = 1$ is favorable for the collision with large impact parameter. In general, the collision with large impact parameter should show greater sensitivity to the change of collision energy than the collision with a small impact parameter. From this sense, the reactivity of the $|M'_J| = 2$ state (the dominant configuration of $|L_Z| = 1$) should more rapidly decrease as the collision energy increases due to the attractive character of the PES, because the fast Ar (^{3}P$_2$) atoms may be less subject to the attractive interaction than the slow Ar (^{3}P$_2$) atoms. However, this general expectation conflicts with the experimental result. Therefore, it is unlikely that the slight difference of the collision energy gives a significant effect on the atomic alignment effect.

Another origin for the different atomic alignment effect on the CF$_3$H beam condition is the difference of the rotational state distribution at two beam conditions. The average values of J and K, $\langle J \rangle$ and $\langle K \rangle$, for two beam conditions are summarized in Table 1. Here J is the total angular momentum and K is the projection of J to the molecular symmetry axis. It is reasonable to attribute this molecular rotation effect to the dissociation dynamics itself in the excited states after the energy transfer has occurred because the energy transfer probability depends only on the electronic term and has little dependence on the internal motion of molecule. To understand the effect of molecular rotation on the atomic alignment effect, we must assume at least two excited states of CF$_3$H that have different molecular rotation dependences on the dissociation dynamics for CF$_3$* formation. This assumption seems to be consistent with our previous report for the molecular orientation effect on the emission spectra of CF$_3$*[15] and the theoretical report for the CF$_3$* emission.[25] On the basis of the theoretical study on the vacuum ultraviolet absorption spectra, two excited states of
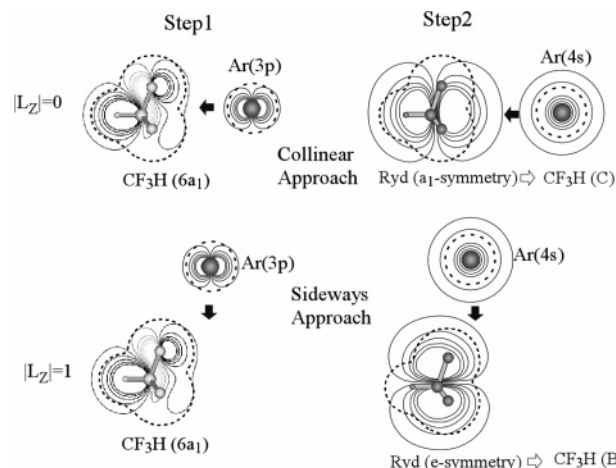

Figure 6. Proposed stereoselectivity in the electron exchange. The final Rydberg state of CF$_3$H has a good correlation with the configuration of the 3p orbital of Ar in the collision frame. In step 1, the $L_Z = 0$ configuration of the 3p orbital is favorable for the collinear approach, and the $|L_Z| = 1$ configuration is favorable for the sideways approach. In step 2, the collinear approach is favorable for the formation of CF$_3$H (C), and the sideways approach is favorable for the formation of CF$_3$H (B).

CF$_3$H, CF$_3$H (B) and CF$_3$H (C), are energetically accessible in the reaction of Ar (^{3}P$_2$) + CF$_3$H.[26,27] These excited states are characterized as the transitions from the 6a$_1$ orbital to the different Rydberg orbitals: 6e and 8e (Ryd 3p) for CF$_3$H (B), 7a$_1$ and 8a$_1$ (Ryd 3p) for CF$_3$H (C). These two excited states correlate to the excited CF$_3$ radicals, CF$_3$*(1E′) and CF$_3$*(2A″), respectively. Because the fluorescence quantum yield in these states has been estimated to be ~17% for the visible emission,[27] the CF$_3$* formation channel is competitive with other dark exit channels. Unfortunately, no information is available for the effect of molecular rotation on the CF$_3$* fluorescence quantum yield in these excited states of CF$_3$H. According to the assumption that the effect of molecular rotation on the atomic alignment dependence can be attributed to the competition between these two excited states, it is strongly expected that the atomic orientation plays an important role for the selectivity of the final Rydberg state of CF$_3$H.

To understand the selectivity of the final Rydberg state of CF$_3$H, we must consider the steric aspect in step 2. According to the symmetry of the Rydberg states, the formation of CF$_3$H (B) should be favorable at the sideways approach because the Rydberg orbitals having e-symmetry can efficiently overlap with the 4s orbital of Ar(^{3}P$_2$). On the other hand, the formation of CF$_3$H (C) is favorable at the collinear approach because the Rydberg orbitals have a$_1$-symmetry. As discussed in section 3.2, the $L_Z = 0$ configuration of 3p orbital should be favorable for the collinear approach from both the CF$_3$-end and H-end directions. On the other hand, the configuration of $|L_Z| = 1$ is expected to be favorable for the collision from the sideways direction. As a result, it is likely that the final Rydberg state of CF$_3$H also has a good correlation with the configuration of the 3p orbital of Ar(^{3}P$_2$) in the collision frame. The proposed stereoselectivity in the electron exchange is summarized in Figure 6. This correlation is well supported by the molecular orientation dependence of the emission spectra previously reported.[15] Therefore, we can at least partly explain the effect of molecular rotation on the atomic alignment effect. Of course, it is, in nature, difficult to explain the experimental results completely by the simple electron exchange model because the atomic alignment effect depends not on L (and its projection L_Z) but on the total angular momentum J (and its projection

Atomic Alignment Dependence in Ar ($^3P_2$) + CF$_3$H

J. Phys. Chem. A, Vol. 111, No. 30, 2007 **6919**

M_J) involving spin effect. As a conclusion, a good correlation between the molecular orientation and the atomic orientation in the energy transfer process is revealed.

References and Notes

(1) Hertel, I. V.; Hofmann, H.; Rost, K. A. *Phys. Rev. Lett.* **1977**, *38*, 343.

(2) Rettner, C. T.; Zare, R. N. *J. Chem. Phys.* **1981**, *75*, 3636.

(3) Schmidt, H.; Bahring, A.; Meyer, E.; Miller, B. *Phys. Rev. Lett.* **1982**, *48*, 1008.

(4) Richter, C.; Dowek, D.; Houver, J. C.; Andersen, N. *J. Phys. B* **1990**, *23*, 3925.

(5) Smith, C. J.; Spain, E. M.; Daiberth, M. J.; Leone, S. R.; Driessen, J. P. J. *J. Chem. Soc., Faraday Trans.* **1993**, *89*, 1401.

(6) Campbell, E. E. B.; Schmidt, H.; Hertel, I. V. *Adv. Chem. Phys.* **1998**, *72*, 37.

(7) Percival, I. C.; Seaton, M. J. *Proc. Soc. Soc.* **1957**, *53*, 654.

(8) Watanabe, D.; Ohoyama, H.; Matsumura, T.; Kasai, T. *J. Chem. Phys.* **2006**, *125*, 084316.

(9) Watanabe, D.; Ohoyama, H.; Matsumura, T.; Kasai, T. *J. Chem. Phys.* **2006**, *125*, 224301.

(10) Matsumura, T.; Ohoyama, H.; Watanabe, D.; Yasuda, K.; Kasai, T. *J. Phys. Chem. A* **2007**, *111*, 3069.

(11) Matsumura, T.; Ohoyama, H.; Watanabe, D.; Yasuda, K.; Kasai, T. *J. Phys. Chem. A* **2007**, in press.

(12) Ohoyama, H.; Kasai, T.; Ohashi, K.; Hirata, Y.; Kuwata, K. *Chem. Phys. Lett.* **1986**, *131*, 20.

(13) Ohoyama, H.; Kasai, T.; Ohashi, K.; Kuwata, K. *Chem. Phys. Lett.* **1987**, *136*, 236.

(14) Ohoyama, H.; Kasai, T.; Kuwata, K. *Chem. Phys.* **1992**, *165*, 155.

(15) Ohoyama, H.; Iguro, T.; Kasai, T.; Kuwata, K. *Chem. Phys. Lett.* **1993**, *209*, 361.

(16) Kawaguchi, H.; Ohoyama, H.; Kasai, T. *Bull. Chem. Soc. Jpn.* **2002**, *75*, 85.

(17) Velazco, J. E.; Kolts, J. H.; Setser, D. W. *J. Chem. Phys.* **1978**, *69*, 4357.

(18) Watanabe, D.; Ohoyama, H.; Matsumura, T.; Kasai, T. *Phys. Rev. Lett.* **2007**, in press.

(19) Zare, R. N. *Angular Momentum*; Wiley: New York, 1998.

(20) Takahashi, H.; Ohoyama, H.; Kasai, T.; Nakano, M.; Yamaguchi, K. *J. Phys. Chem.* **1995**, *99*, 13600.

(21) Setser, D. W.; Dreiling, T. P.; Brashers, H. C.; Kolts, J. H. *Faraday Discuss. Chem. Soc.* **1979**, *67*, 255.

(22) Ohno, K.; Mutoh, H.; Harada, Y. *J. Am. Chem. Soc.* **1983**, *105*, 4555.

(23) Mulliken, R. S. *J. Chim. Phys.* **1949**, *46*, 497.

(24) Ohno, K. *Bull. Chem. Soc. Jpn.* **2004**, *77*, 887.

(25) Washida, N.; Suto, M.; Nagase, S.; Nagashima, U.; Morokuma, K. *J. Chem. Phys.* **1983**, *78*, 1025.

(26) Biehl, H.; Boyle, K. J.; Tuckett, R. P.; Baumgärtel, H.; Jochims, H. W. *Chem. Phys.* **1997**, *214*, 367.

(27) Suto, M.; Lee, L. C. *J. Chem. Phys.* **1983**, *79*, 1127.